Carbohydrate Polymers 106 (2014) 42–48

Contents lists available at ScienceDirect

Carbohydrate Polymers

journal homepage: www.elsevier.com/locate/carbpol

# Preparation, antiangiogenic and antitumoral activities of the chemically sulfated glucan from *Phellinus ribis*

Yuhong Liu[a,b,c], Yuguo Liu[d], Haiqiang Jiang[b], Lingchuan Xu[b], Yanna Cheng[e], Peng George Wang[c], Fengshan Wang[a,c,*]

[a] *Key Laboratory of Chemical Biology of Natural Products (Ministry of Education), Institute of Biochemical and Biotechnological Drug, School of Pharmaceutical Sciences, Shandong University, Jinan 250012, China*
[b] *School of Pharmaceutical Sciences, Shandong University of Traditional Chinese Medicine, Jinan 250355, China*
[c] *National Glycoengineering Research Center, Shandong University, Jinan 250012, China*
[d] *Department of Pharmacy, Shandong Tumor Hospital, Jinan 250117, China*
[e] *Department of Pharmacology, School of Pharmaceutical Sciences, Shandong University, Jinan 250012, China*

ARTICLE INFO

*Article history:*
Received 28 September 2013
Received in revised form 25 January 2014
Accepted 27 January 2014
Available online 4 February 2014

*Keywords:*
Sulfated derivatives
Antiangiogenesis
Antitumoral activity
β-Glucan
*Phellinus ribis*

ABSTRACT

Two sulfated derivatives (PRP-S1 and PRP-S2) of a β-glucan from *Phellinus ribis* with different degrees of substitution were obtained by chlorosulfonic acid method. The derivatives could block formation of new vessels in zebrafish and inhibit the proliferation of human umbilical vein endothelial cells (HUVECs). The two sulfated derivatives had remarkably high antitumor activities *in vivo* (in BALB/c mice inoculated with H22 hepatocellular carcinoma) as well as *in vitro* (against human ovary cancer SKOV-3 cells), without producing any overt signs of general toxicity. The results of immunohistochemistry assay indicated that the derivatives significantly reduced the average number of microvessel density (MVD) and inhibited the expression of vascular endothelial growth factor (VEGF) in tumor. Thus, these derivatives exhibit pronounced antiangiogenic and antitumoral properties. Except for cytotoxic effects on tumor cells, it is reasonable to expect that the antitumoral effects of PRP-S1 and PRP-S2 are mediated *via* their antiangiogenic properties.



## 1. Introduction

Angiogenesis, the formation of new vessels from preexisting microvascular networks, plays a crucial role in tumor progression (Hanahan & Folkman, 1996; Makrilia, Lappa, Xyla, Nikolaidis, & Syrigos, 2009). In cancer, new vessel formation contributes to the progressive growth and metastasis of solid tumors (Bergers & Benjamin, 2003; Ichihara, Kiura, & Tanimoto, 2011), making antiangiogenesis an important strategy in cancer therapeutics.

Recently, antiangiogenic activities have been increasingly reported in a number of sulfated polysaccharides, including acharan sulfate (a new type of glycosaminoglycan from the giant African snail) (Ghosh et al., 2002), arabinogalactan sulfate (Xu, Dong, Qiu, Cong, & Ding, 2010), a sulfated polysaccharide from *Antrodia cinnamomea* (Cheng, Chang, Chao, & Lu, 2012) and a chemically sulfated heteropolysaccharide from *Sepiella maindroni* ink (Zong et al., 2013). There is now clear evidence that recognition of cell-surface heparan sulfate, with a structure similar to that of sulfated polysaccharides, is required for growth factor actions during angiogenic processes (Cohen et al., 1995; Vlodavsky, Miao, Medalion, Danagher, & Ron, 1996). All these have generated a surge of interest in the development of sulfated polysaccharide-based antiangiogenesis and antitumor agents.

Polysaccharide of *Phellinus ribis* (PRP), a β-D-glucan with a mean molecular weight of 8.59 kDa, was isolated from the fruiting bodies of *P. ribis* in our previous work (Liu & Wang, 2007). The predicted structure was shown in Fig. 1. It contains a (1→4), (1→6)-linked backbone, with a single β-D-glucose at the C-3 position of (1→6)-linked glucosyl residue every eight residues along the main chain. PRP has an obvious immunostimulating effect, but has no antitumor activity. In view of antiangiogenic activities of the above-mentioned sulfated polysaccharides, we prepared two sulfated PRP derivatives by chemical modification and studied their antiangiogenic and antitumoral activities.

* Corresponding author at: Institute of Biochemical and Biotechnological Drug, Key Laboratory of Chemical Biology of Natural Products (Ministry of Education), School of Pharmaceutical Sciences, Shandong University, Jinan 250012, Shandong, PR China. Tel.: +86 531 88382589; fax: +86 531 88382548.
*E-mail addresses:* fswang@sdu.edu.cn, wangfengshansdu@hotmail.com (F. Wang).

0144-8617/$ – see front matter © 2014 Elsevier Ltd. All rights reserved.
http://dx.doi.org/10.1016/j.carbpol.2014.01.088

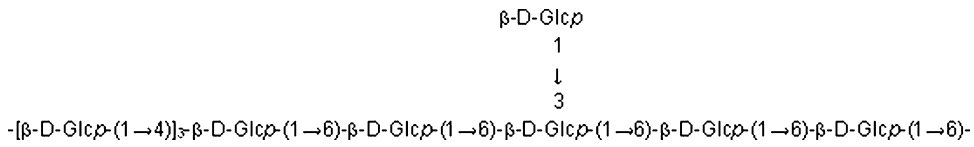


**Fig. 1.** Predicted structure of polysaccharide PRP isolated from *Phellinus ribis*.

## 2. Materials and methods

### 2.1. Materials

*P. ribis* was collected from mountain areas in Jinan, Shandong Province, China in October 2009. Chlorosulfonic acid was produced in Guoyao Institute of Chemical Engineering in Shanghai. Formamide was from Beijing Yili Co. Ltd., China. DEAE-Sepharose Fast Flow was from Pharmacia Co. (Sweden). Dulbecco's modified Eagle's medium (DMEM) and fetal bovine serum (FBS) were purchased from Gibco-BRL, Life Technologies Inc., USA. 3-(4,5-Dimethylthiazol-2-yl)-2,5-diphenyltetrazolium bromide (MTT) was purchased from Sigma Chemicals Co., USA. The rabbit anti-mouse vascular endothelial growth factor (VEGF) and CD34 polyclonal antibodies were from Boster Biological Technology Co. Ltd., Wuhan, China. Immunohistochemical kits were purchased from Zhongshan Golden Bridge Biotechnology Co. Ltd., Beijing, China. All other reagents were of analytical grade made in China.

### 2.2. Sulfation of PRP

PRP was obtained by the method reported previously (Liu & Wang, 2007). Sulfation of PRP was carried out using the chlorosulfonic acid method (Yoshida, Yasuda, Mimura, & Kaneko, 1995). In brief, PRP sample (200 mg) was suspended in anhydrous formamide (2 ml) at room temperature with stirring for 30 min and then the sulfating reagent (2 ml) (Lu, Wang, Hu, Huang, & Wang, 2008) was added dropwise. The mixture was maintained at 30 °C for 6 h with continuous stirring. After the reaction was finished, the mixture was cooled, neutralized with 2.5 M NaOH solution, and treated by adding ethanol. The resulting precipitate was redissolved in water and dialyzed against distilled water. The retained nondialysate was treated with ethanol again. The precipitate was dissolved in water, applied to DEAE-Sepharose Fast Flow column (2.6 cm × 20 cm), and eluted with water and NaCl solution with a concentration gradient of 0–2.0 M. Based on the colorimetric test for total carbohydrate by phenol-sulfuric acid method (Dubois, Gilles, Hamilton, Rebers, & Smith, 1956), the main fraction was collected, dialyzed and lyophilized to give sulfated PRP. Two sulfated derivatives (PRP-S1 and PRP-S2) with different degrees of substitution (DS) were obtained by varying the ratio of chlorosulfonic acid to formamide in the sulfating reagent (Table 1) under constant reaction conditions.

### 2.3. Characterization

Optical rotation was measured at 20 °C with a WZZ-1 polarimeter. FT-IR spectra (KBr pellets) were recorded on a Nicolet Nexus 470 FT-IR spectrophotometer. Elemental analysis (C, H, S) was conducted on a Perkin-Elmer 2400 instrument.

The homogeneity and molecular weight of the sulfated derivatives were determined by high-performance gel-permeation chromatography (HPGPC) on a Waters 515 instrument equipped with an Ultrahydrogel 250 column (7.8 mm × 300 mm) and a Waters 2410 Refractive Index Detector (RID). Twenty microliters (20 μl) of sample solution (0.5% PRP-S solution) was injected in each run, with 0.05 M $Na_2SO_4$ as the mobile phase at a flow rate of 0.8 ml/min. The HPGPC system was pre-calibrated with T-series Dextran standards (T-10, T-20, T-40, T-70, T-110 and T-500).

### 2.4. Antiangiogenesis assay with zebrafish

Green fluorescent protein (GFP) transgenic zebrafish embryos (Institute of Biology, Shandong Academy of Sciences, China) were maintained at 28 °C on a 14 h light/10 h dark cycle. All embryos were generated by natural pair-wise mating and staged as previously described (Kimmel, Ballard, Kimmel, Ullmann, & Schilling, 1995). Four to five pairs were set up for each mating, and on average 100–150 embryos per pair were generated. Embryos were maintained in embryo water (5 g of Instant Ocean Salt in 25 L of distilled water, pH 7.4) at 28 °C for 20 h until the 21 somite stage before sorting for viability using both morphology and developmental stage as criteria. Healthy embryos were dechorionated by enzymatic digestion with 1 mg/ml protease for 5 min at room temperature.

Embryo water or samples dissolved in embryo water were transferred into a 96-well plate with 200 μl per well. Wells without samples were included as blank controls. One healthy embryo at 20 h post-fertilization was added to each well. The 96-well plate was maintained at 28 °C on a 14 h light/10 h dark cycle. After incubation for another 52 h, morphological changes in intersegmental vessels (ISVs) of the zebrafish were observed and the intact ISVs were counted under the COIC XSZ-H fluorescence microscope (Chongqing Photoelectric Instrument Co. Ltd., China). The inhibitory rate (IR) was calculated according to the formula below:

$$\text{IR}\ (\%) = \left(1 - \frac{\text{ISVs amount of experimental group}}{\text{ISVs amount of blank control}}\right) \times 100$$

### 2.5. Cell proliferation assay

Human umbilical vein endothelial cells (HUVECs) were isolated from human umbilical cord veins by 0.1% type-I collagenase digestion at 37 °C for 15 min. HUVECs were maintained in DMEM medium containing 10% heat-inactivated FBS and 3 ng/ml of bFGF. Human ovary cancer SKOV-3 cells were obtained from Shandong

**Table 1**
Characterization of PRP-S1 and PRP-S2.

| PRP-S[a] | CSA:FA[b] | Yield (mg) | $\bar{M}_w$ (kDa) | $[\alpha]_D^{20}$ | Elemental analysis (%) | | | DS |
|---|---|---|---|---|---|---|---|---|
| | | | | | C | H | S | |
| PRP-S1 | 1:6 | 237 | 14.69 | +8.75° | 22.80 | 3.74 | 9.73 | 0.96 |
| PRP-S2 | 1:3 | 263 | 18.32 | +2.38° | 17.79 | 2.98 | 12.81 | 1.62 |

[a] From the parent PRP 200 mg.
[b] The ratio of chlorosulfonic acid to formamide in sulfating reagent.

Academy of Medical Sciences, China. The growth inhibition effects of the sulfated derivatives on cells were evaluated with MTT colorimetric assay. Cells were collected and seeded in a 96-well plate at $1.0 \times 10^4$ cells/well, with a volume of 190 μl in DMEM medium with 10% FBS. The cells were incubated for 24 h at 37 °C in a humidified 5% $CO_2$ incubator. Subsequently, various concentrations of PRP, PRP-S1 and PRP-S2 were added. Wells without PRP or PRP-S treatment were included as blank controls. After incubation for another 48 h, 10 μl of MTT (5 mg/ml) was added into each well and incubated for another 4 h. The supernatant was removed carefully, and 150 μl of DMSO was added to each well. The absorbance at 570 nm was measured with an ELISA reader (Bio-Rad Model 6800, USA). The IR was calculated according to the formula below:

$$\text{IR}\ (\%) = \left(1 - \frac{\text{Absorbance of experimental group}}{\text{Absorbance of blank control group}}\right) \times 100$$

### 2.6. Antitumor activity in vivo and tumor angiogenesis inhibition assay

#### 2.6.1. Animals and treatment

The use of female BALB/c mice (6–8 weeks old, 18–20 g) was approved by the Institutional Animal Care Committee of Shandong University and we strictly followed the Ethical Guidelines for the Care and Use of Animals. Ninety mice were randomly divided into nine groups, 10 animals per group. One group served as normal control group. Hepatocellular carcinoma ascites (0.2 ml, $2 \times 10^6$ cells) of 7 days old were transplanted subcutaneously into the right axilla of each mouse of the rest eight groups. The mice were treated as following: normal control group (saline); model control group (saline); four PRP-S groups (PRP-S1:10, 20 mg/kg body weight; PRP-S2: 10, 20 mg/kg body weight); two PRP groups (PRP:10, 20 mg/kg body weight); positive control group (cyclophosphamide, 20 mg/kg body weight). All the groups were administered by intraperitoneal injection in 0.2 ml every day for 10 days, starting 24 h after tumor implantation.

#### 2.6.2. Tumor weight, thymus and spleen index

Twenty-four hours after the last drug administration, the mice were sacrificed by cervical dislocation. Spleen, thymus and tumor weights of the mice were measured. The antitumor activity *in vivo* was expressed as an IR calculated as $[(A - B)/A] \times 100\%$, where $A$ and $B$ were the average tumor weight of the model control and experimental group, respectively.

#### 2.6.3. Immunohistochemistry assay

The H22 tumor specimens were separated from muscle, fixed in 10% formalin solution and then embedded with paraffin. The paraffin embedded tumor samples were cut into 8-μm sections, then dewaxed in xylene and rehydrated through graded concentrations of ethanol. Antigen retrieval was performed by heating slides in a microwave oven in citrate buffer. Endogenous peroxide was blocked by treating slides in 3% $H_2O_2$ in methanol for 30 min at 37 °C. Primary antibody (VEGF or CD34 antibody) was then added and the sections were incubated overnight at 4 °C. After the incubation of biotin-labeled secondary antibody, slides were stained with diaminobenzidine (DAB) substrate and counterstained with hematoxylin. The specimens were first viewed at low magnification (×40 or ×100), then positive staining was counted in a ×200 field and five randomly chosen fields per section were selected to determine the average count of microvessel density (MVD) (Weidner, 1995). Any single highlighted endothelial cell, an endothelial cell cluster clearly separated from adjacent microvessels, or distinct clusters of brownstaining endothelial cells were counted as a separate count. The evaluation of the expression level of VEGF was performed in accordance with the immunoreactive score (IRS) (Friedrichs, Gluba, & Editmann, 1993): IRS = SI (staining intensity) × PP (percentage of positive cells). SI was determined as 0, negative; 1, weak; 2, moderate; and 3, strong. PP was defined as 0, negative; 1, 10% positive cells; 2, 11%–50% positive cells; 3, 51–80% positive cells; and 4, more than 80% positive cells.

### 2.7. Statistical analysis

The data obtained were expressed as mean ± SD and analyzed using ANOVA method. Significance of any differences between groups was evaluated using Student's *t*-test.

## 3. Results and discussion

### 3.1. Sulfation of PRP and characterization

Sulfated PRP was synthesized by chlorosulfonic acid method. Two sulfated derivatives named PRP-S1 and PRP-S2 were obtained by varying the ratio of chlorosulfonic acid to formamide in sulfating reagent. Their DS (DS means the amount of mole of sulfur per mole of glucose residue) were calculated according to the ratio of carbon to sulfur by element analysis (Yoshida et al., 1995), as shown in Table 1. Both PRP-S1 and PRP-S2 showed a symmetrical peak on HPGCP, and the average molecular weights of PRP-S1 and PRP-S2 were determined to be 14.69 and 18.32 kDa, respectively,

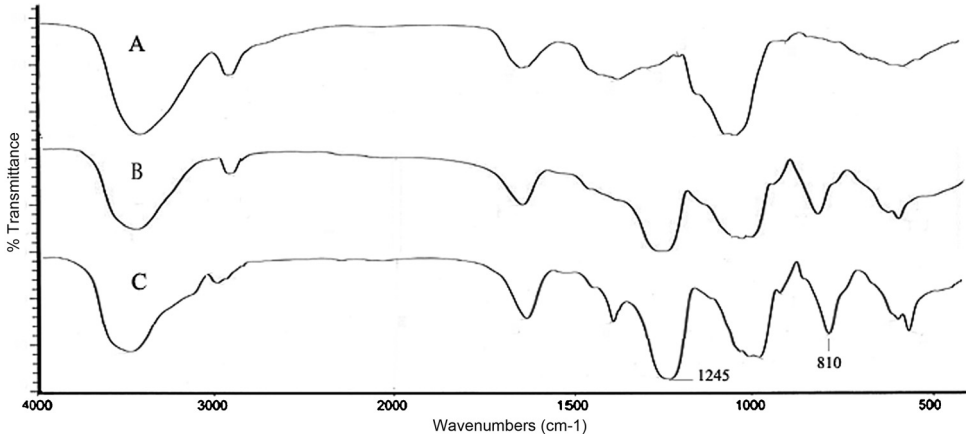


**Fig. 2.** FI-IR spectra of (A) PRP, (B) PRP-S1 and (C) PRP-S2.

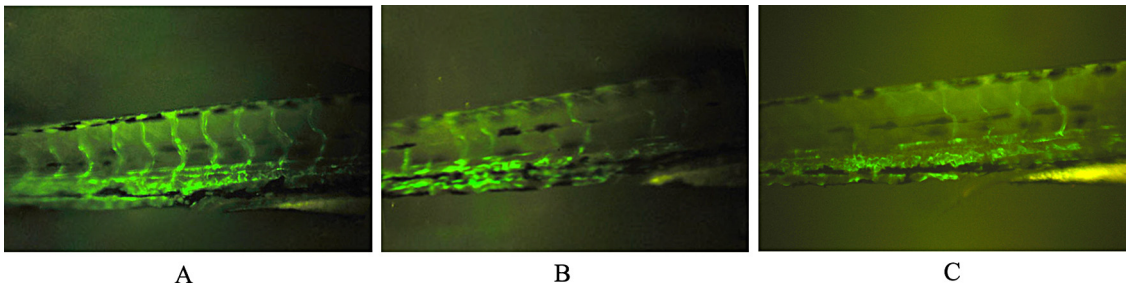


**Fig. 3.** The intersegmental vessels of zebrafish (partial enlarged view). (A) Blank control; (B) PRP-S1 (100 μM); (C) PRP-S2 (100 μM).

indicating that nearly no degradation occurred in the sulfation reaction process.

As shown in Fig. 2, PRP sulfates showed two characteristic absorption bands in FT-IR, one at near 1245 $cm^{-1}$ describing an asymmetrical S=O stretching vibration and the other at near 810 $cm^{-1}$ representing a symmetrical C—O—S vibration associated with a C–O–$SO_3$ group, indicating incorporation of the sulfate group. These results suggested that PRP-S1 and PRP-S2 were successfully sulfated (Liu et al., 2013).

### 3.2. Inhibitory effect of the sulfated derivatives on zebrafish angiogenesis

Zebrafish has become a well accepted model for screening molecules that affect blood vessel formation. Zebrafish blood vessels form by angiogenic sprouting and appear to require the same proteins that are necessary for blood vessel growth in mammals. Zebrafish provides the relevance of an *in vivo* environment as well as the potential for high throughput drug screening (Cross, Cook, Lin, Chen, & Rubinstein, 2003; Simmich, Staykov, & Scott, 2012). Thus, zebrafish angiogenesis assay was first carried out to determine whether the sulfated derivatives displayed antiangiogenic activity.

The effects of the sulfated derivatives on angiogenesis in zebrafishes were assessed by morphological observation (Fig. 3) and a quantitative analysis of ISVs (Table 2). As shown in Fig. 3, ISVs of the zebrafishes in blank control group were clear and intact, whereas, some ISVs of the zebrafishes treated with the sulfated derivatives were damaged or lost. Both PRP-S1 and PRP-S2 caused statistically significant dose-dependent decreases in the amount of ISVs (PRP-S1: 18.28 at 100 μM, 22.13 at 50 μM, 24.88 at 10 μM; PRP-S2: 16.39 at 100 μM, 20.33 at 50 μM, 23.56 at 10 μM) in zebrafishes (amount of ISVs in blank control: 28.23) (Table 2). The results indicated that PRP-S1 and PRP-S2 could inhibit the angiogenesis of zebrafishes.

### 3.3. Effects of the sulfated derivatives on HUVECs proliferation

Blood vessels can be formed by the proliferation and migration of vascular endothelial cells. As the sulfated derivatives showed antiangiogenic activity in zebrafish assay, we evaluated effects of PRP-S1, PRP-S2 and PRP on the proliferation of HUVECs by MTT assay. The results were shown in Fig. 4(A). It was found that PRP had no obvious influence on HUVECs, but the sulfated derivatives exhibited distinct inhibition effect on the proliferation of HUVECs in a dose-dependent manner. At the doses of 10 μM, 25 μM, and 50 μM, the inhibitory rates of PRP-S1 were 23.9%, 32.9%, and 35.3%, respectively, and the inhibitory rates of PRP-S2 were 30.4%, 44.1%, and 53.3%, respectively. The result implied that the sulfated derivatives inhibited angiogenesis perhaps by the means of inhibiting HUVECs growth.

### 3.4. Effects of the sulfated derivatives on SKOV-3 cell proliferation

It was reported that chemical sulfation of polysaccharides might lead to antitumor activity (Wei, Wei, Cheng, & Zhang, 2012; Zhang, Liu, Park, Xia, & Kim, 2012; Zhua et al., 2013). In this study, the *in vitro* growth inhibitory effects of PRP-S1, PRP-S2 and PRP against human ovary cancer SKOV-3 cells were also examined. The results, as shown in Fig. 4(B), indicated that PRP did not suppress the cell' growth, but the sulfated derivatives could inhibit the proliferation of SKOV-3 cells, with the inhibitory rates of 17.2%, 20.8%, and 25.7% for PRP-S1 at 10 μM, 25 μM, and 50 μM, and 25.4%, 28.0%, and 30.3% for PRP-S2 at 10 μM, 25 μM, and 50 μM, respectively. The sulfated derivatives showed inhibitory effects against both HUVECs and SKOV-3 cells; however, HUVECs cells seemed to be more sensitive to PRP-S1 and PRP-S2 than SKOV-3 cells when comparing their inhibitory rates at the same concentration.

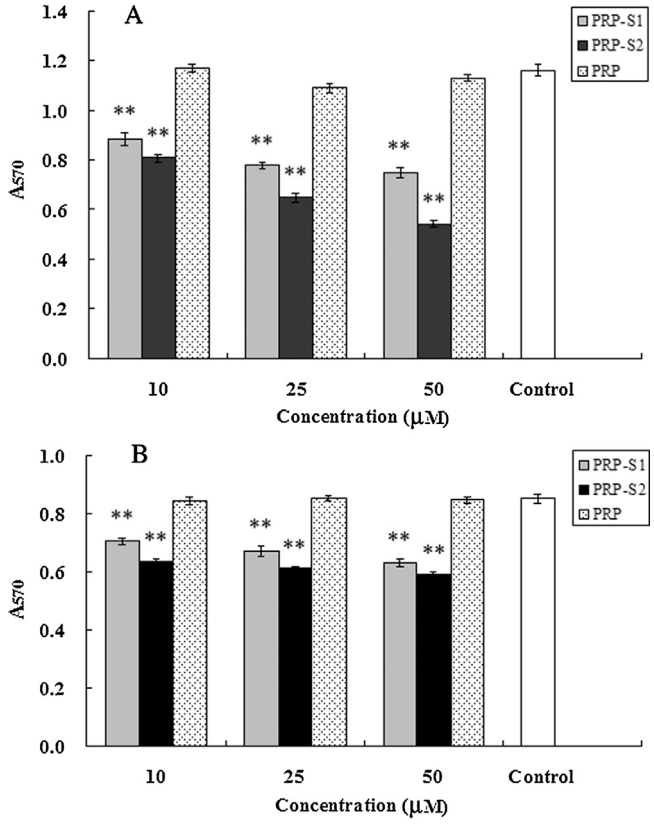


**Fig. 4.** Effects of PRP-S1, PRP-S2 and PRP on cell proliferation. (A) Human umbilical vein endothelial cells (HUVECs). (B) Human ovary cancer SKOV-3 cells. Activity was expressed as the absorption at 570 nm. Values are means ± SD, $n = 6$, $^{**}P < 0.01$ *vs.* control group.

**Table 2**
Effects of PRP-S1 and PRP-S2 on zebrafish angiogenesis.

| Group | Result | $C$ (μM) | | |
|---|---|---|---|---|
| | | 10 | 50 | 100 |
| PRP-S1 | Amount of ISVs[a] | 24.88 ± 1.13* | 22.13 ± 1.09** | 18.28 ± 0.94** |
| | IR (%)[b] | 11.87 | 21.61 | 35.25 |
| PRP-S2 | Amount of ISVs[a] | 23.56 ± 1.31* | 20.35 ± 1.17** | 16.39 ± 0.88** |
| | IR (%)[b] | 16.54 | 27.91 | 41.94 |
| Blank control | Amount of ISVs[a] | 28.23 ± 0.89 | | |

[a] Intact intersegmental vessels and the data were expressed as mean ± SD ($n$ = 10).
[b] IR was calculated as (1 − ISVs amount of experimental group/ISVs amount of blank control) × 100%.
* $P$ < 0.05 *vs.* blank control.
** $P$ < 0.01 *vs.* blank control.

**Table 3**
Effects of PRP-S1, PRP-S2 and PRP on the spleen index, thymus index and tumor weight of tumor-bearing mice.

| Group[a] | Dose (mg/kg) | Spleen index[b] (mg/g) | Thymus index[c] (mg/g) | Tumor weight (g) | Inhibitory rate[d] (%) |
|---|---|---|---|---|---|
| Normal control | – | 5.98 ± 1.14 | 2.65 ± 0.73 | – | – |
| Model control | – | 5.67 ± 0.93 | 2.41 ± 0.41 | 1.03 ± 0.18 | – |
| PRP-S1 | 10 | 5.61 ± 1.01 | 2.83 ± 0.59 | 0.58 ± 0.11** | 43.2 |
| | 20 | 5.95 ± 1.09 | 2.59 ± 0.53 | 0.47 ± 0.08** | 54.6 |
| PRP-S2 | 10 | 5.85 ± 0.87 | 2.77 ± 0.62 | 0.53 ± 0.07** | 48.7 |
| | 20 | 5.86 ± 0.97 | 2.57 ± 0.46 | 0.41 ± 0.09** | 60.6 |
| PRP | 10 | 6.23 ± 1.18 | 2.61 ± 0.39 | 0.92 ± 0.13 | 10.7 |
| | 20 | 7.95 ± 0.99* | 3.70 ± 0.47** | 0.83 ± 0.10 | 19.4 |
| Positive control | 20 | 3.87 ± 0.78* | 1.04 ± 0.29** | 0.25 ± 0.07** | 75.7 |

Values are means ± SD ($n$ = 10).
[a] Model control, positive control and sample groups were inoculated with H22 hepatocellular carcinoma, while normal control was not. Normal and model controls received saline intraperitoneally, while positive control was administered cyclophosphamide.
[b] Spleen index was measured as the ratio of the spleen weight (mg) to body weight (g).
[c] Thymus index was measured as the ratio of the thymus weight (mg) to body weight (g).
[d] Tumor inhibitory rate was calculated as $[(A - B)/A] \times 100\%$, where $A$ and $B$ were the average tumor weight of the model control and experimental group, respectively.
* $P$ < 0.05 *vs.* model control.
** $P$ < 0.01 *vs.* model control.

### 3.5. Antitumoral activity in vivo

As the sulfated derivatives showed antiangiogenic activity in zebrafish and inhibitory effect against tumor cell proliferation *in vitro*, we further investigated the antitumoral effect of PRP-S1 and PRP-S2 compared with PRP *in vivo*. The results (Table 3) showed that PRP could enhance spleen and thymus index in H22-bearing mice at dose of 20 mg/kg, suggesting a strong immunostimulatory activity. PRP also inhibited the growth of tumor to some extent when compared with model control, but the difference did not prove a statistical significance. However, a significant tumor inhibition effect was observed from the tumor-bearing mice treated with PRP-S1 and PRP-S2. At the doses of 10 and 20 mg/kg, the inhibitory rates of PRP-S1 were 43.2% and 54.6%, and the inhibitory rates of PRP-S2 were 48.7% and 60.6%, respectively. Cyclophosphamide (positive control) decreased spleen and thymus indices considerably in H22-bearing mice, although it had a high inhibitory rate (75.7%) at a dose of 20 mg/kg. It was worth noting that treatment of PRP-S1 and PRP-S2 did not induce any deaths or body weight loss (data not shown), and it did not influence spleen and thymus indices (Table 3), suggesting a relatively low adverse reaction.

### 3.6. Inhibitory effect of the sulfated derivatives on tumor angiogenesis

It is now generally accepted that tumor angiogenesis is crucial both for the growth of a primary neoplastic tumor and for the development of metastasis. Although angiogenesis is difficult to measure directly in human tumors, it is suggested that quantification of immunohistochemically stained microvessels density (MVD) in histological sections may be used as an index (Weidner, Semple, Welch, & Folkman, 1991). The most common antibodies used for microvessel staining so far are against Von Willebrand Factor (Factor VIII), CD31, CD34, and recently CD105 (Schimming & Marme, 2002).

To clarify if the tumor inhibition was partially due to the antiangiogenic function of the sulfated derivatives, we assessed MVD by immunohistochemistry assay for CD 34. As shown in Fig. 5(A)–(C), abundant capillary-like nets were found in the sections from the model control group, while only a few were observed in the sections from mice treated with PRP-S1 and PRP-S2. Angiogenesis was quantified by counting the number of positive microvessels. As shown in Table 4, compared to that of the model control group, the average number of MVD in the PRP-S-treated mice was reduced in a dose-dependent pattern.

**Table 4**
Effects of PRP-S1 and PRP-S2 on MVD and VEGF in H22 hepatoma in mice.

| Group | Dose (mg/kg) | MVD[a] | VEGF[b] |
|---|---|---|---|
| Model control | – | 27.09 ± 4.40 | 8.21 ± 1.15 |
| PRP-S1 | 10 | 19.07 ± 3.67* | 6.23 ± 0.69* |
| | 20 | 17.45 ± 3.06** | 6.06 ± 0.73** |
| PRP-S2 | 10 | 18.01 ± 3.12** | 5.97 ± 0.81** |
| | 20 | 15.98 ± 2.98** | 4.57 ± 0.52** |

Values are means ± SD ($n$ = 10).
[a] Microvessel density.
[b] Vascular endothelial growth factor.
* $P$ < 0.05 *vs.* model control.
** $P$ < 0.01 *vs.* model control.

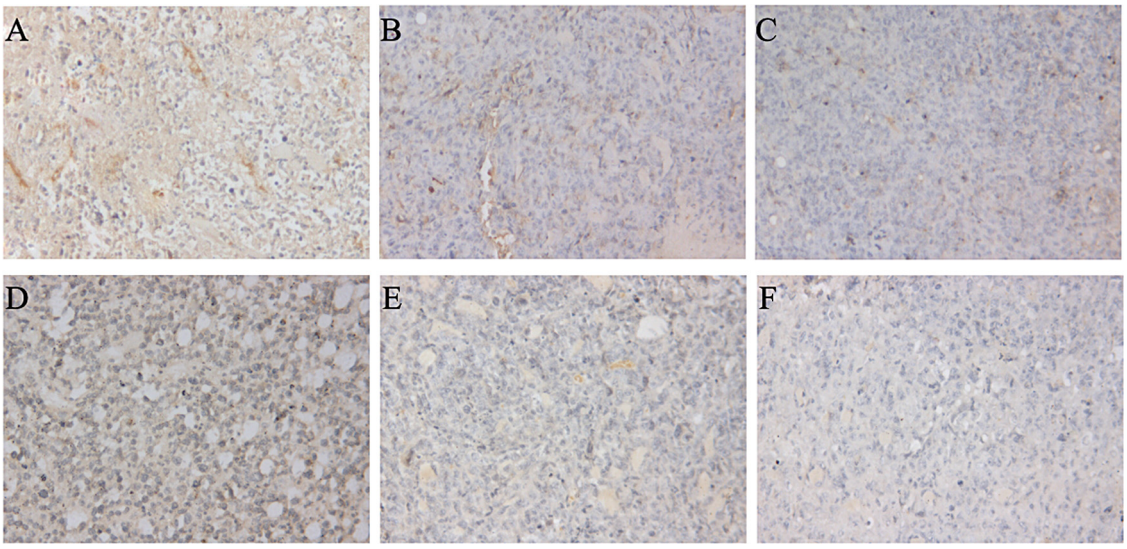


**Fig. 5.** Immunohistochemical staining of H22 tumor sections. The quantification of MVD with CD34 antibody in (A) Model control, (B) PRP-S1 (20 mg/kg), and (C) PRP-S2 (20 mg/kg). VEGF expression in (D) Model control, (E) PRP-S1 (20 mg/kg) and (F) PRP-S2 (20 mg/kg).

### 3.7. Effects of the sulfated derivatives on VEGF expression

Among the factors causing tumor angiogenesis, VEGF is considered as a leading candidate (Schmitt & Matei, 2012). It induces the proliferation, differentiation, and migration of vascular endothelial cells, increases the permeability of the capillaries, and enhances the survival of endothelial cells by preventing their apoptosis (Breslin, Pappas, Cerveira, Hobson, & Duran, 2003; Reinmuth et al., 2003). It has been demonstrated that the level of VEGF is frequently up-regulated in tumor tissues, and the overexpression of VEGF enhances tumor growth and metastasis and is associated with poor clinical outcomes (Shweiki, Itin, Soffer, & Keshet, 1992; Zhang et al., 1995).

In the present work, we investigated the expression of VEGF in H-22 tumor using immunohistochemical analysis. As shown in Fig. 5(D)–(F), a strong immunoreactivity of VEGF was observed in model control group, whereas VEGF immunostain was weak in PRP-S groups. A quantitative analysis (Table 4) showed that both PRP-S1 and PRP-S2 considerably inhibited the expression of VEGF in tumor at the doses of 10 and 20 mg/kg. The results suggested that PRP-S inhibited angiogenesis of tumor by down-regulating VEGF expression.

In recent years, treatment targeting angiogenesis has been a hot topic in cancer research. PRP-S1 and PRP-S2, two sulfated derivatives of a polysaccharide from traditional Chinese medicine, were found to have antiangiogenic activity in the present study. Moreover, they could inhibit the growth of tumor in mice, without producing any overt signs of general toxicity (such as body weight loss or immune function decline). Therefore, we reasonably expect that the mechanisms of the antitumoral effects of PRP-S1 and PRP-S2 are mediated, at least in part, *via* their antiangiogenic properties.

## 4. Conclusions

Two sulfated derivatives of PRP from *P. ribis* were prepared by chlorosulfonic acid method. The derivatives display antiangiogenic and antitumoral properties which might be instrumental for the control of diseases associated with angiogenic dysfunction. Nonetheless, the full chemical structures of the derivatives, as well as the mechanisms underlying their actions, remain to be characterized.

## Acknowledgments

This work was supported by grants from the Youth Scientist Foundation of Shandong Province (BS2009SW041), the "973" grant from the Ministry of Science and Technology of China (2012CB822102), Research Fund for the Doctoral Program of Higher Education of China (20103731120004) and Taishan scholar Scheme (Special Term Expert for Pharmacy).

## References

Bergers, G., & Benjamin, L. E. (2003). Tumorigenesis and the angiogenesis switch. *Nature Reviews Cancer*, *3*, 401–410.

Breslin, J. W., Pappas, P. J., Cerveira, J. J., Hobson, R. W., & Duran, W. N. (2003). VEGF increases endothelial permeability by separate signaling pathways involving ERK-1/2 and nitric oxide. *American Journal of Physiology: Heart and Circular Physiology*, *284*, 92–100.

Cheng, J. J., Chang, C. C., Chao, C. H., & Lu, M. K. (2012). Characterization of fungal sulfated polysaccharides and their synergistic anticancer effects with doxorubicin. *Carbohydrate Polymers*, *90*, 134–139.

Cohen, T., Gitay-Goren, H., Sharon, R., Shibuya, M., Halaban, R., Levi, B., et al. (1995). VEGF121, a vascular endothelial growth factor (VEGF) isoform lacking heparin binding ability, requires cell-surface heparan sulfates for efficient binding to the VEGF receptors of human melanoma cells. *Journal of Biological Chemistry*, *270*, 11322–11326.

Cross, L. M., Cook, M. A., Lin, S., Chen, N., & Rubinstein, A. L. (2003). Rapid analysis of angiogenesis drugs in a live fluorescent zebrafish assay. *Arteriosclerosis, Thrombosis, and Vascular Biology*, *23*, 911–912.

Dubois, M., Gilles, K. A., Hamilton, J. K., Rebers, P. A., & Smith, F. (1956). Colorimetric method for determination of sugars and related substances. *Analytical Chemistry*, *28*, 350–356.

Friedrichs, K., Gluba, S., Editmann, H., & Jonat, W. (1993). Overexpression of P53 and prognosis in breast cancer. *Cancer*, *72*, 3641–3647.

Ghosh, A. K., Hirasawa, N., Lee, Y. S., Kim, Y. S., Shin, K. H., & Ryu, N. K. (2002). Inhibition by acharan sulphate of angiogenesis in experimental inflammation models. *British Journal of Pharmacology*, *137*, 441–448.

Hanahan, D., & Folkman, J. (1996). Patterns and emerging mechanisms of the angiogenic switch during tumorigenesis. *Cell*, *86*, 353–364.

Ichihara, E., Kiura, K., & Tanimoto, M. (2011). Targeting angiogenesis in cancer therapy. *Acta Medica Okayama*, *65*, 353–362.

Kimmel, C. B., Ballard, W. W., Kimmel, S. R., Ullmann, B., & Schilling, T. F. (1995). Stages of embryonic development of the zebrafish. *Development Dynamics*, *203*, 253–310.

Liu, C., Chen, H., Chen, K., Gao, Y., Gao, S., Liu, X., et al. (2013). Sulfated modification can enhance antiviral activities of *Achyranthes bidentata* polysaccharide against porcine reproductive and respiratory syndrome virus (PRRSV) in vitro. *International Journal of Biological Macromolecules*, *52*, 21–24.

Liu, Y., & Wang, F. (2007). Structural characterization of an active polysaccharide from *Phellinus ribis*. *Carbohydrate Polymers*, *70*, 386–392.

Lu, Y., Wang, D., Hu, Y., Huang, X., & Wang, J. (2008). Sulfated modification of epimedium polysaccharide and effects of the modifiers on cellular infectivity of IBDV. *Carbohydrate Polymers*, *71*, 180–186.

Makrilia, N., Lappa, T., Xyla, V., Nikolaidis, I., & Syrigos, K. (2009). The role of angiogenesis in solid tumours: An overview. *European Journal of Internal Medicine*, *20*, 663–671.

Reinmuth, N., Parikh, A., Ahmad, S. A., Liu, W., Stoeltzing, O., Fan, F., et al. (2003). Biology of angiogenesis in tumors of the gastrointestinal tract. *Microscope Research Techniques*, *60*, 199–207.

Schimming, R., & Marme, D. (2002). Endoglin (CD105) expression in squamous cell carcinoma of the oral cavity. *Head Neck*, *24*, 151–156.

Schmitt, J., & Matei, D. (2012). Targeting angiogenesis in ovarian cancer. *Cancer Treatment Reviews*, *38*, 272–283.

Shweiki, D., Itin, A., Soffer, D., & Keshet, E. (1992). Vascular endothelial growth factor induced by hypoxia may mediate hypoxia-initiated angiogenesis. *Nature*, *359*, 843–845.

Simmich, J., Staykov, E., & Scott, E. (2012). Zebrafish as an appealing model for optogenetic studies. *Progress in Brain Research*, *196*, 145–162.

Vlodavsky, I., Miao, H., Medalion, B., Danagher, P., & Ron, D. (1996). Involvement of heparan sulfate and related molecules in sequestration and growth promoting activity of fibroblast growth factor. *Cancer Metastasis Reviews*, *15*, 177–186.

Wei, D., Wei, Y., Cheng, W., & Zhang, L. (2012). Sulfated modification, characterization and antitumor activities of *Radix hedysari* polysaccharide. *International Journal of Biological Macromolecules*, *51*, 471–476.

Weidner, N. (1995). Current pathologic methods for measuring intratumoral microvessel density within breast carcinoma and other solid tumors. *Breast Cancer Research and Treatment*, *36*, 169–180.

Weidner, N., Semple, J. P., Welch, W. R., & Folkman, J. (1991). Tumor angiogenesis and metastasis – Correlation in invasive breast carcinoma. *New England Journal of Medicine*, *324*, 1–8.

Xu, Y., Dong, Q., Qiu, H., Cong, R., & Ding, K. (2010). Structural characterization of an arabinogalactan from *Platycodon grandiflorum* roots and antiangiogenic activity of its sulfated derivative. *Biomacromolecules*, *11*, 2558–2566.

Yoshida, T., Yasuda, Y., Mimura, T., & Kaneko, Y. (1995). Synthesis of curdlan sulfates having inhibitory effects in vitro against AIDS viruses HIV-1 and HIV-2. *Carbohydrate Research*, *276*, 425–436.

Zhang, H. T., Craft, P., Scott, P. A., Marina, Z., Weich, H. A., Harris, A. L., et al. (1995). Enhancement of tumor growth and vascular density by transfection of vascular endothelial cell growth factor into MCF-7 human breast carcinoma cells. *Journal of National Cancer Institute*, *87*, 213–219.

Zhang, J., Liu, Y., Park, H., Xia, Y., & Kim, G. (2012). Antitumor activity of sulfated extracellular polysaccharides of *Ganoderma lucidum* from the submerged fermentation broth. *Carbohydrate Polymers*, *87*, 1539–1544.

Zhua, Z., Liu, Y., Si, C., Yuan, J., Lv, Q., Li, Y., et al. (2013). Sulfated modification of the polysaccharide from *Cordyceps gunnii mycelia* and its biological activities. *Carbohydrate Polymers*, *92*, 872–876.

Zong, A., Zhao, T., Zhang, Y., Song, X., Shi, Y., & Cao, H. (2013). Anti-metastatic and anti-angiogenic activities of sulfated polysaccharide of *Sepiella maindroni* ink. *Carbohydrate Polymers*, *91*, 403–409.